

DATA-DRIVEN BASED IMC CONTROL

JOSÉ DAVID ROJAS AND RAMÓN VILANOVA

Departament de Telecomunicació i Enginyeria de Sistemes
Universitat Autònoma de Barcelona
08193, Bellaterra, Spain
{josedavid.rojas; ramon.vilanova}@uab.cat

Received December 2010; revised June 2011

ABSTRACT. *In this paper, a new data-driven methodology for the Internal Model Control controller tuning based on the Virtual Reference Feedback Tuning method is presented. Taking advantage of the characteristics of the Internal Model Control structure, a robustness test is presented and analyzed using only the available data taken in an open-loop experiment. Examples are provided to show the application of this technique using a non-linear plant.*

Keywords: Data driven control, Internal model control, Polymerization reaction, Virtual reference feedback tuning

1. **Introduction.** New control methodologies based only on experimental data have recently appeared in literature. These methodologies skip the modeling step and find the controller directly from one or more experiments on the plant. The Iterative Feedback Tuning (IFT) [1, 2] computes an unbiased gradient of a performance index to improve iteratively the tuning of the parameters of a reduced order discrete time controller. The Correlation-based Tuning (CbT) [3] is a one-shot methodology that attempts to find the values of a restricted order controller that minimizes the correlation between the closed-loop error of the system (based in a desired closed-loop behavior) and the reference signal. The Virtual Reference Feedback Tuning (VRFT) [4] translates the model reference control problem into an identification problem, being the controller the transfer function to identify. The optimization used to find the parameters of the controllers is based on some “virtual signals” computed from a batch of data taken directly from an open-loop experiment. The Fictitious Reference Iterative Tuning (FRIT) is a method similar to the VRFT, but, instead of an open-loop experiment, it deals with closed-loop data, taking into account the original controller [5, 6, 7]. These methodologies are good examples of this new trend in control that attempts to find the restricted order controller using an experimental data based optimization problem.

One of the drawbacks of data-driven control is that the “classical” stability analysis cannot be performed, since a model of the process is needed. Concepts of robustness like “phase margin” and “gain margin” [8] are not directly applicable in data-driven design. Recently, some results have appeared in the literature which include some stability constraints in the optimization problem for the CbT [9]. This stability condition is based on the infinity norm of an error function and depends on the frequency content and the number of samples of the data. Added to the stability conditions, a way to measure the robustness on data-driven controllers is desirable. One of the model-based control methods that introduces the idea of robustness in the design of controllers is Internal Model Control (IMC) [10, 11]. In this paper, the conjunction of the VRFT methodology with the robustness condition of IMC is presented, unifying the best of two worlds.

IMC is a very popular and well known method [12] that explicitly uses a model of the plant as integral part of the control structure. The literature on IMC is broad and many extensions to the original framework have been presented. For example, in [13], the internal model of the controller is adaptively updated on-line with provable guarantee of stability. One of the interesting characteristics of IMC control is that the controller can be expressed as a PID-like controller if the model of the plant has certain characteristics. A complete presentation of the relationship between IMC and PID control can be found in [14] while in [15] IMC is applied to PI/PID controllers to study the interactions between loops for a MIMO plant. In [16], neural networks are used to approximate both the model of the plant as well as the controller.

IMC has been recognized as an appropriate paradigm to face a robust design. Therefore, it is technically sound to adopt such framework and embed it in a data-driven design approach. This is a novel feature and the main contribution of this paper is to show how two conceptually opposite approaches can combine together in order to face a model-free based robust design. An overview of the IMC and the IMC-VRFT method are presented in Section 2. A robust stability test is introduced and a design procedure is proposed in Sections 3 and 4. The methodology is tested in an academic example as well as in a non-linear plant in Section 5. An analysis of the factors that affects the robust stability test is presented in Section 6 to close the paper.

2. Using Data for the Internal Model Control Methodology.

2.1. Overview of the internal model control. The standard control structure is depicted in Figure 1. $P(z)$ represents the Plant, while $\bar{P}(z)$ is its model. $Q(z)$ is the IMC controller. In the absence of disturbances, the control acts as if it was open-loop control for the reference tracking, but when a disturbance enters to the system, the same controller acts as closed-loop for the disturbance rejection. If $Q(z)$ is designed as $Q(z) = P(z)^{-1}f(z)$ and $\bar{P}(z) = P(z)$, the output becomes

$$y = f(z)r + (1 - f(z))d \quad (1)$$

It is clear that, to have perfect model matching control (in closed-loop, the desired dynamics are given by $f(z)$), $Q(z)$ must try to cancel the dynamics of the plant. This characteristics leads to the well know property that an IMC system would be nominally internally stable if $Q(z)$ is stable, in case the model is equal to the plant. Finding a perfect model is rarely achievable and if it were, $Q(z)$ may not be possible to contain the inverse of this model due to physical limitations or because the inverse of the plant may lead to an unstable controller. In [11], a two-step design is proposed for this kind of controller:

1. Solve the nominal performance criterion given, for example, by

$$\min_{Q(z)} \|(1 - \bar{P}(z)\bar{Q}(z))W(z)\|_p \quad (2)$$

where $W(z)$ is a filter chosen to give more importance in certain frequencies and $\|\cdot\|_p$ is a given norm that defines the performance criterion. The optimal solution of this problem yields to a sensitivity function given by $S^*(z) = 1 - \bar{P}(z)\bar{Q}(z)$ and the complementary sensitivity function given by $M^*(z) = \bar{P}(z)\bar{Q}(z)$, that is, the response to a change in the reference is as if it were in open loop, while the response to a disturbance is in closed-loop.

2. To introduce robustness considerations, the complementary sensitivity has to be rolled off at high frequencies, therefore, it is necessary to add a low pass filter $f(z)$

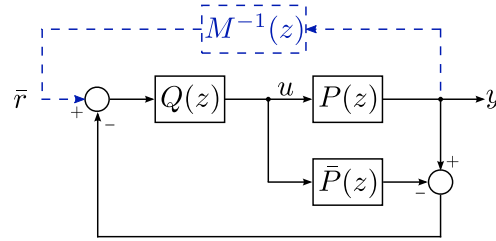


FIGURE 1. Standard structure of the IMC. $\bar{P}(z)$ represents the plant model and $Q(z)$ is the IMC controller. The dashed line represents the virtual signal for the VRFT procedure.

to the controller $\bar{Q}(z)$, to obtain the final controller $Q(z) = \bar{Q}(z)f(z)$. Suppose that the multiplicative uncertainty is bounded by a frequency dependent function $\bar{l}_m(\omega)$,

$$\left| \frac{P(e^{j\omega}) - \bar{P}(e^{j\omega})}{\bar{P}(e^{j\omega})} \right| \leq \bar{l}_m(\omega)$$

The closed-loop system is robustly stable if and only if

$$|f(e^{j\omega})| < \frac{1}{|\bar{P}(e^{j\omega})\bar{Q}(e^{j\omega})\bar{l}_m(\omega)|} \quad \forall \omega \tag{3}$$

IMC control has become very popular because, finding the controller and the conditions for robust stability can be cast in a very simple form. As seen in (1), the $Q(z)$ controller just need to be set as the best approximation of the inverse of the model multiplied by a filter that defines the desired behavior in closed-loop. In addition to this, under certain conditions on the model of the plant, the final controller (the combination of $Q(z)$ and $\bar{P}(z)$) can be rewritten as a PID controller, allowing to use the IMC method directly to tune this kind of controllers, which are widely used in industry [17].

Having a good model and an approximation of the uncertainty is vital for IMC. Since the model is an integral part of the controller, in this paper the use of data-driven control is proposed to jump from the data to the controller directly and to use the same information to find an approximation of the uncertainty. The VRFT is the selected framework for this task, given its flexibility to apply the “virtual signal” idea into different structures.

2.2. The IMC-VRFT. VRFT is a data driven, one shot control methodology that translates a control problem into an identification problem using only data taken from the plant itself [4, 18]. Starting from a batch of open-loop input-output data $\{u(t), y(t)\}$, a “virtual” signal is computed in such a way that, if the closed-loop system is feed with this virtual signal and the controllers in the loop were the ideal controllers that would achieve a predefined target transfer function, then the input and output signals of the plant in closed-loop would be the same than the batch of open-loop data.

Several extension to the original VRFT have appeared in the literature. In [19], the tuning of the feedback controller to match a defined sensitivity function is presented; in [20], the two degrees of freedom controller case is tackled; in [21], a feedforward controller is added to decouple the tuning of the reference tracking and the disturbance rejection problem; in [22], some extension and stability test are presented for the single controller case.

In the case of IMC, in Figure 1, the experimental setup is depicted. If the target complementary sensitivity function is given by $M(z)$, then the virtual reference $\bar{r}(t)$ is computed as

$$\bar{r}(t) = M^{-1}(z)y(t) \tag{4}$$

From Figure 1, it can be found that the ideal controller would be given by

$$\begin{aligned} Q_0(z) &= M(z)P^{-1}(z) \\ \bar{P}_0(z) &= M(z)Q_0^{-1}(z) \end{aligned} \quad (5)$$

where $P_0(z)$ is the ideal plant model that is derived from the ideal controller. This basic idea leads to the following optimization problem which gives the set of optimal parameters θ^* (in a least square sense):

$$\min_{\theta} J(\theta) = \min_{\theta} \sum_{i=1}^N (u(i) - Q(z, \theta)\bar{r}(i))^2 \quad (6)$$

Once $Q(z, \theta^*)$ has been determined, it is easy to compute the approximation of the process model of the plant from (5):

$$\bar{P}(z, \theta^*) = M(z)Q^{-1}(z, \theta^*) \quad (7)$$

It is important to note that $\bar{P}(z, \theta)$ is seen just as an “instrumental model”, that results from the determination of the optimal controller. This instrumental model is used as part of the control loop and, as presented in the next section, as the manner to describe a “nominal plant”. In data-driven control, there is no nominal model of the plant, therefore, to define a test to check if the controller is robustly stable, it is necessary to approximate the plant by this “instrumental model”. The filter for robust operation presented in (3), is already included in $Q(z, \theta^*)$ since the closed-loop behavior is expected to be $M(z)$, but it is not possible to know if condition (3) is fulfilled just by solving this optimization problem. It is, therefore, desirable to have a data-based test to check if this condition holds.

3. Robust Stability for the IMC-VRFT. When the closed-loop system is stable for all perturbed plants about the nominal model up to the worst-case model uncertainty, it is said that the system has robust stability [23]. In data-driven control, it is difficult to find a controller that assures robust stability of the plant since not even a nominal model is available (in [24], the stability problem is addressed by adding some constraints in the frequency domain directly into the optimization problem). However, it is possible to use (3) and the batch of input-output data, to test if the controller is robustly stabilizing the plant, before the actual controller is implemented, by approximating the uncertainty function $\bar{l}_m(\omega)$.

Using the results on *Empirical Transfer Function Estimate* (ETFTE) from [25], given an input-output set of N points of data $\{u(t), y(t)\}_N$ from a plant $G(z)$ which transfer function is suppose to be unknown, the estimate of the frequency response $\hat{G}_N(e^{j\omega})$ is given by

$$\hat{G}_N(e^{j\omega}) = \frac{Y_N(\omega)}{U_N(\omega)} \quad (8)$$

where $U_N(\omega)$ and $Y_N(\omega)$ are given by

$$\begin{aligned} U_N(\omega) &= \frac{1}{\sqrt{N}} \sum_{t=1}^N (u(t)e^{-j\omega t}) \\ Y_N(\omega) &= \frac{1}{\sqrt{N}} \sum_{t=1}^N (y(t)e^{-j\omega t}) \end{aligned} \quad (9)$$

The essential points are given in $\omega = 2\pi k/N$, $k = 0, 1, \dots, N-1$. Other points are obtained by interpolation. For example, in Figure 2, the comparison between the real

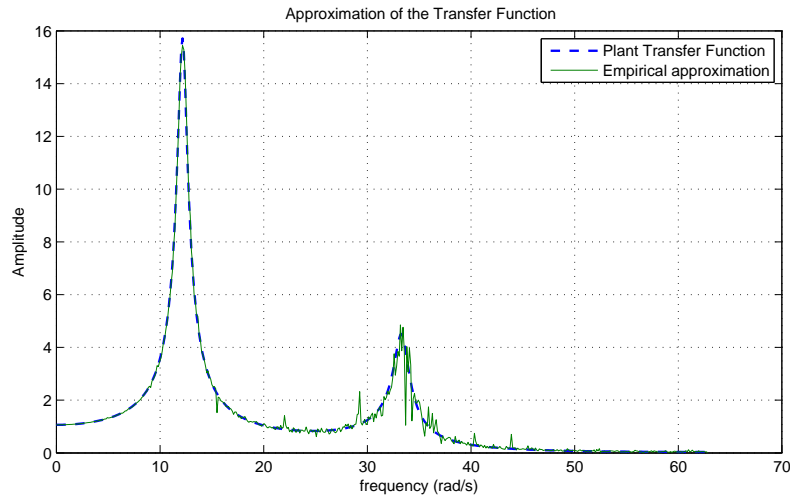


FIGURE 2. Approximation of the transfer function using open-loop data

frequency response and the empirical approximation is presented using a set of 1024 point of a PRBS signal on the plant given in [4],

$$\begin{aligned}
 P(z) &= \frac{A(z)}{B(z)} \\
 A(z) &= 0.2826z^{-3} + 0.5067z^{-4} \\
 B(z) &= 1 - 1.418z^{-1} + 1.589z^{-2} \\
 &\quad - 1.316z^{-3} + 0.8864z^{-4}
 \end{aligned} \tag{10}$$

with sampling time $t_s = 0.05$ s. As it can be seen the approximation is fairly good even for the resonant peaks.

According to [25], the ETFE is an asymptotically unbiased estimate of the transfer function at increasingly (with N) many frequencies, but the variance of the ETFE do not decrease as N increases. That is why, in Figure 2, the ETFE seems to be “noisy”.

To tackle this problem, the use of filtering windows is recommended to smooth the ETFE. Other techniques can be use to find the approximation of the transfer function. For example, in [26], a time-frequency analysis is applied to estimate the dynamics of an F-18 system research aircraft. The data is cleaned manually using a time-frequency plot and then the Fourier transform is applied to find the transfer function. In [27, 28], an adaptive algorithm is proposed to use variable bandwidth windowing centered at different frequencies in order to smooth the ETFE. The computational effort is bigger than with standard ETFE, but the compromise between bias and variance is solved. In [29] and references therein, neural networks are used to approximate the Geophysical Model Function (the transfer function of a scatterometer) in order to use real data to determine the wind vectors over the ocean. In the following, the ETFE is applied to approximate the uncertainty function of the controlled system. How to compute the ETFE, is important, but does not change the core idea of the algorithm, which is one of the main contribution of the paper.

3.1. Approximation of $\bar{l}_m(\omega)$ and the robust stability test. If the function $\bar{l}_m(\omega)$ can be approximated using the ETFE, it will be possible to perform a data-based test to check Robust Stability using (3). In the case of the IMC-VRFT, the assumption on the instrumental model $\bar{P}(z)$ is that it is close enough to the real plant transfer function, in order to left the “nominal” stability depending on $Q(z)$: if $Q(z)$ is stable, the “nominal”

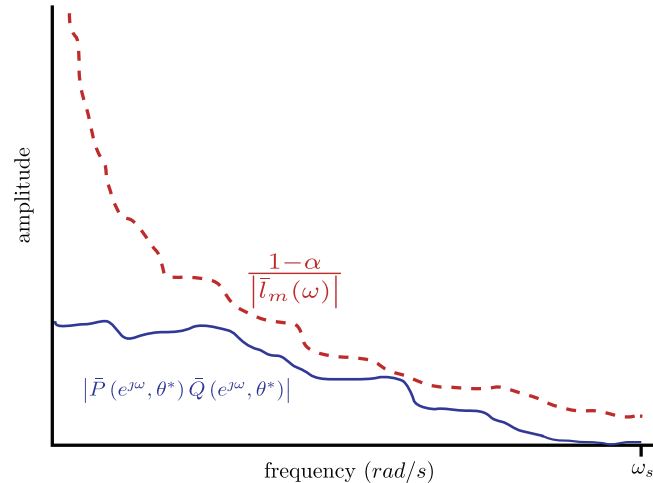


FIGURE 3. Graphical Interpretation of the robust stability test

closed-loop system is stable given that the plant is stable. If the controller has been found using the proposed approach, the filter is already included in $Q(z)$ and (3) can be rewritten as

$$\left| \hat{P}(e^{j\omega}, \theta^*) \hat{Q}(e^{j\omega}, \theta^*) \bar{l}_m(\omega) \right| \leq 1 \quad (11)$$

or, if a “security” constant $\alpha \geq 0$ is added to cope with possible errors when approximating \bar{l}_m

$$\left| \hat{P}(e^{j\omega}, \theta^*) \hat{Q}(e^{j\omega}, \theta^*) \bar{l}_m(\omega) \right| \leq 1 - \alpha \quad (12)$$

A graphical interpretation of (12) can be seen in Figure 3: if at some point the dashed line falls below the solid line (which represents the complementary sensitivity function if the instrumental model is close enough to the transfer function of the plant) it means one is trying to extend the system beyond the limits uncertainty allows. At this point (12) fails, and it is not possible to assure robust stability with controller $Q(z, \theta^*)$ and given value of α .

To approximate (12), the frequency response of $Q(z, \theta^*)$ and $\bar{P}(z, \theta^*)$ can be calculated using the results of the optimization. $\bar{l}_m(\omega)$ is approximated using the definition of the multiplicative uncertainty and the ETFE approximation. The test can be stated as in Table 1. If the test failed, the designer has two options: it is possible to increase the number of parameters of the controller or to relax the closed-loop specification $M(z)$. Once the new controller is found, the test can be performed again to check if the robust condition holds for the new setting.

4. Controller Design Procedure. Using the tuning method of Section 2 and the robust test of Section 3, it is possible to derive a design procedure for the VRFT-IMC controller:

1. Collect a set of open-loop input-output data $\{u(t), y(t)\}_N$.
2. Define a desired closed-loop transfer function $M(z)$. It is a common practice to define $M(z)$ as first order and use the settling time as a design parameter. If it is possible to determine the settling time of the system from the data (for example if the experimental data contains a step change in the input), a rule of thumb is to set the closed-loop settling time to be less than 10 times faster the open-loop settling time. Also select the parameterization of $Q(z, \theta)$.
3. Find the controller $Q(z, \theta)$ and the instrumental model $\bar{P}(z, \theta)$ according to the methodology presented in Section 2.2 and solving (6) and (7).

TABLE 1. Robust stability test algorithm

Require: Find N points of input-output open-loop data from the plant: $\{u(t), y(t)\}_N$

Require: Define a value for α such as $\alpha \geq 0$

Require: Find $Q(z, \theta^*)$ and $\bar{P}(z, \theta^*)$, $Q(z, \theta^*)$ and $\bar{P}(z, \theta^*)$ have to be stable

Require: Define a set of frequencies ω

- 1: Compute $y_{diff}(t)$ as $y_{diff}(t) = y(t) - \bar{P}u(t)$
- 2: Compute $y_{model}(t)$ as $y_{model}(t) = \bar{P}u(t)$
- 3: Compute $\hat{G}_{diffN}(e^{j\omega})$ using $y_{diff}(t)$ as the output and $u(t)$ as the input with (8)
- 4: Compute $\hat{P}_N(e^{j\omega})$ using $y_{model}(t)$ as the output and $u(t)$ as the input with (8)
- 5: Compute $\bar{l}_m(\omega) = \frac{abs(\hat{G}_{diffN}(e^{j\omega}))}{abs(\hat{P}_N(e^{j\omega}))}$
- 6: **for** each ω **do**
- 7: **if** $\left| \hat{P}(e^{j\omega}, \theta^*) \hat{Q}(e^{j\omega}, \theta^*) \bar{l}_m(\omega) \right| \leq 1 - \alpha$ **then**
- 8: $failRobust(\omega) = 0$ (The system has Robust Stability for the given ω)
- 9: **else**
- 10: $failRobust(\omega) = 1$ (It is not possible to assure robust stability)
- 11: **end if**
- 12: **end for**

4. Compute algorithm 1 to check if the controllers are robust. If the test fails, then go back to 2, and relax the settling time of $M(z)$ or change the parameterization of $Q(z, \theta)$.

Following this procedure, it is possible to find a robust IMC controller using a single batch of input-output data from the plant.

5. Application Examples. In this section, two examples are presented to show the application of the IMC-VRFT and the Robust Stability Test.

5.1. Example 1: flexible transmission system. This example is used in [4] to present the original VRFT. The plant is the same as in (10) and the target closed-loop transfer function is given by

$$M(z) = \frac{z^{-3}(1 - \alpha)^2}{(1 - \alpha z^{-1})^2}, \quad \alpha = e^{-T_s \bar{\omega}}, \quad \bar{\omega} = 10 \quad (13)$$

where $\bar{\omega} = 10$ rad/s is the desired bandwidth, $T_s = 0.05$ s. This plant has a non-minimum phase zero which could make the optimization to yield an unstable controller. With a PRBS input of 1024 samples, and if the number of controller parameters is left to be enough to find the ideal controller, both the normal VRFT [4] and the IMC-VRFT find the ideal controllers. For the normal VRFT, no filter where used. For a presentation on how to find suitable filters for the VRFT method please refer to [4].

The response when the unstable pole of the controller is removed from both controllers is presented in Figure 4. As expected, the response degrades since the controllers are not equal to the ideal ones. In this case, the sum of absolute errors gives 0.94118 for the normal VRFT while the IMC-VRFT gives 0.64193. This difference results from the fact that, for the IMC-VRFT case, the non-minimum phase behavior of the plant is considered in the instrumental model even when the unstable pole is subtracted from the controller, this is not the case of the normal VRFT where this information is completely removed from the controller.

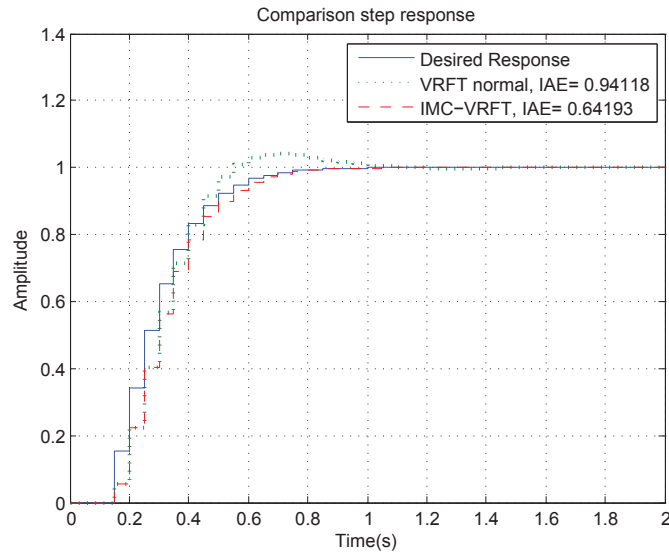


FIGURE 4. Comparison between the normal VRFT and the IMC VRFT after the unstable pole is removed from the controller

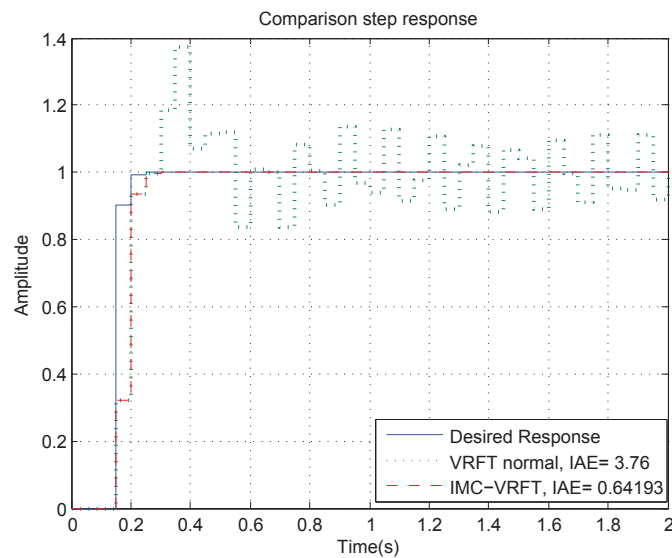


FIGURE 5. Response for $\bar{\omega} = 60$ rad/s

If the desired bandwidth is extended to $\bar{\omega} = 60$ rad/s, the response to a step change of both VRFT approaches and the Robust Stability Test ($\alpha = 0$) are as presented in Figure 5 and Figure 6 respectively. In Figure 5, one can see that the normal VRFT is very sensitive to the change in the desired bandwidth while in the IMC case, since the ideal model is achieved with the parameterization, the response continues to show good performance and, according to the Stability Test, stability is achieved (Figure 6). If for example, there is a mismatch between the model and the plant (in this case, if the instrumental model is computed using the $Q(z)$ after the unstable pole has been removed), the Robust Stability Test is as shown in Figure 7 for $\bar{\omega} = 60$, the closed-loop response is equal to the normal VRFT response in Figure 5. From this example, it is clear that the “quality” of the instrumental model is important to achieve good results, even if controller Q is not exactly equal to the ideal one.

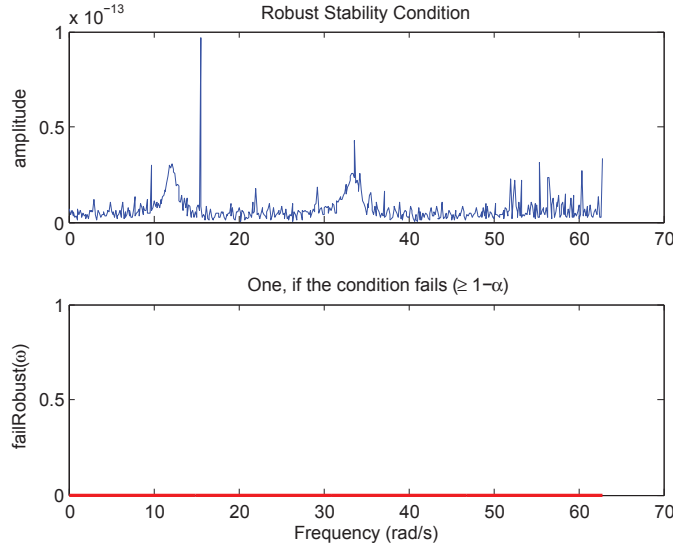


FIGURE 6. Stability test for $\bar{\omega} = 60$ rad/s

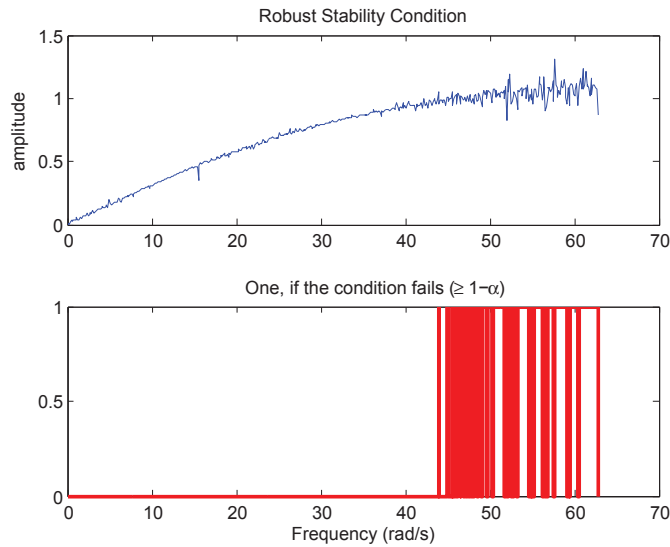


FIGURE 7. Robust stability test with a mismatch between the instrumental model and the plant

5.2. **Example 2: continuous polymerization reaction.** The plant for this example is a polymerization reaction that takes place in a jacketed CSTR. This plant is a 4 states non-linear plant used in [30] for a PID-like Adaptive VRFT control. The model for simulation is given by

$$\begin{aligned}
 \frac{dC_m}{dt} &= -(k_P + k_{fm})C_m P_0 + \frac{F(C_{min} - C_m)}{V} \\
 \frac{dC_I}{dt} &= -k_I C_I + \frac{F_I C_{Iin} - F C_I}{V} \\
 \frac{dD_0}{dt} &= (0.5k_{TC} + k_{Td})P_0^2 + k_{fm}C_m P_0 - F D_0 \\
 \frac{dD_1}{dt} &= M_m(k_P + k_{fm})C_m P_0 - \frac{F D_1}{V}
 \end{aligned}
 \tag{14}$$

TABLE 2. Steady state condition of the polymerization reactor

Steady state operating condition	
$C_m = 5.506774 \text{ kmol/m}^3$	$D_1 = 49.38182 \text{ kmol/m}^3$
$C_I = 0.132906 \text{ kmol/m}^3$	$u = 0.016783 \text{ m}^3/\text{h}$
$D_0 = 0.0019752 \text{ kmol/m}^3$	$y = 25000.5 \text{ kg/kmol}$

TABLE 3. Model parameters of the polymerization reactor

Model parameters	
$k_{Tc} = 1.3281 \times 10^{10} \text{ m}^3/(\text{kmol h})$	$F = 1.00 \text{ m}^3/\text{h}$
$k_{Td} = 1.0930 \times 10^{11} \text{ m}^3/(\text{kmol h})$	$V = 0.1 \text{ m}^3$
$k_I = 1.0225 \times 10^{-1} \text{ L/h}$	$C_{Iin} = 8.0 \text{ kmol/m}^3$
$k_p = 2.4952 \times 10^6 \text{ m}^3/(\text{kmol h})$	$M_m = 100.12 \text{ kg/kmol}$
$k_{fm} = 2.4522 \times 10^3 \text{ m}^3/(\text{kmol h})$	$C_{min} = 6.0 \text{ kmol/m}^3$
$f^* = 0.58$	

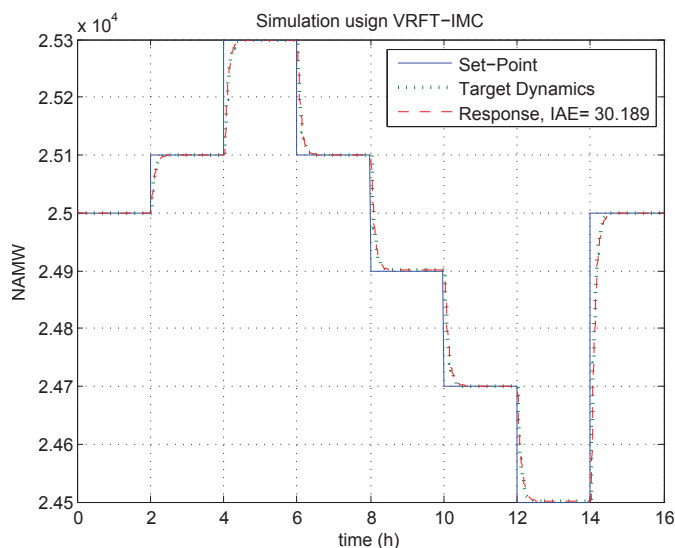


FIGURE 8. Response of the polymerization reaction using the IMC-VRFT. The negative real part of the poles were eliminated from controller Q .

where $P_0 = \sqrt{\left(\frac{2fk_I C_I}{k_{Td} + k_{Tc}}\right)}$ and $y = \frac{D_1}{D_0}$. The parameters for the plant model are presented in Table 2 and Table 3 for completeness. The control objective is to regulate the product number average molecular weight (y) by manipulating the flow rate of the initiator (FI). The procedure followed is the same as in the previous example. However, here an additional filter ($F_{rip}(z)$) was added to $Q(z)$ in order to eliminate the intersample rippling, i.e. eliminating the poles with negative real part of the controller (see [11]). The result of the application of the IMC-VRFT control in the operation point $u = 0.016783 \text{ m}^3/\text{h}$, $y = 25000.5 \text{ kg/kmol}$ is presented in Figure 8. The batch of open loop data was collected using a random Gaussian signal as the input to the plant. The resulting controller and instrumental model became

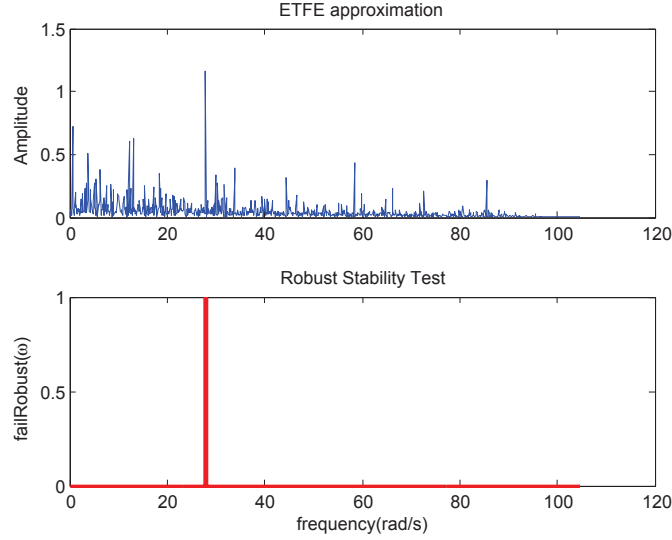


FIGURE 9. Robust stability test done over the polymerization plant

$$\begin{aligned}
 Q(z) &= \frac{-1.238 \times 10^{-5} + 9.593 \times 10^{-6} z^{-1}}{1 + 0.7578 z^{-1}} \\
 \bar{P}(z) &= \frac{-0.28 z^{-1} - 0.2122 z^{-2}}{\left(\begin{array}{c} 1.238 \times 10^{-5} - 1.851 \times 10^{-5} z^{-1} \\ + 6.907 \times 10^{-6} z^{-2} \end{array} \right)} \\
 F_{rip}(z) &= 0.5689 + 0.4311 z^{-1}
 \end{aligned} \tag{15}$$

with a sampling time $T_s = 0.03$ s. In the neighborhood of $y = 25000.5$ kg/kmol the response of the closed-loop system is almost equal to the specified desired response which is given by

$$M(z) = \frac{0.28 z^{-1}}{1 - 0.72 z^{-1}} \tag{16}$$

The stability test is presented in Figure 9 for $\alpha = 0$. As it can be seen, only a point is over 1, representing that one may not be able to guarantee the robust stability. If the desired response is made slower $M(z) = \frac{0.15 z^{-1}}{1 - 0.85 z^{-1}}$, the test results as presented in Figure 10, meaning that robustness is achieved. But it is important to note that since this test is dependent on the input-output data, a single point may be misleading to say that the result is not robustly stabilizing since it could be a false positive because of certain approximation error, due to the inherent variance of the ETFE.

6. Analysis of the Robust Test. In this section, the analysis of the effect of different factors over the robust test are presented. First the sensitivity of the test due to the data is presented, as well as the effect of the choice of the closed loop transfer function and the number of parameters of the controller $Q(z)$. To analyze the test, a second order discrete time plant was chosen:

$$P(z) = \frac{0.01867 z^{-1} + 0.01746 z^{-2}}{1 - 1.783 z^{-1} + 0.8187 z^{-2}} \tag{17}$$

The sampling time was chosen as $T_s = 0.1$ s.

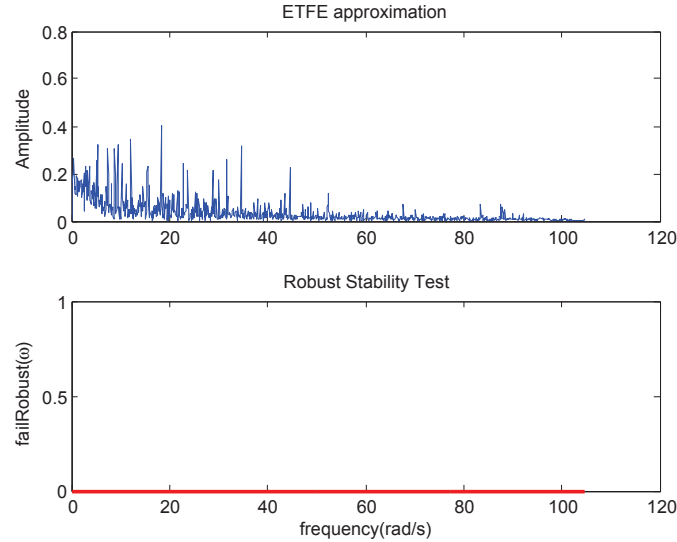


FIGURE 10. Robust stability test done over the polymerization plant with a slower desired response

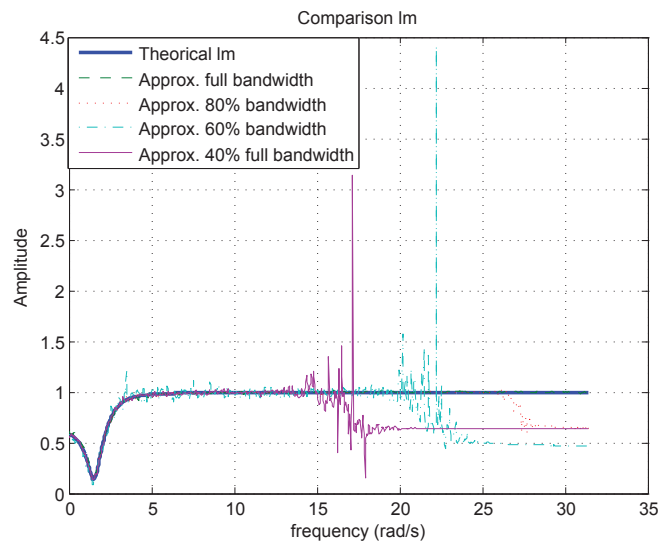


FIGURE 11. Approximation of the ETFE with different inputs

6.1. Effect of the data. In Figure 11, the effect of different input-output data is presented for the approximation of $\bar{l}_m(\omega)$. In all cases, the IMC controller was selected as a simple gain $Q(z) = q_0$ and the closed-loop function was selected as:

$$M(z) = \frac{0.9516z^{-1}}{1 - 0.9048z^{-1}} \quad (18)$$

The difference between each case is the frequency content of the input signal. A 100% bandwidth data is defined as a random gaussian input data that has frequency components up to half the sampling frequency, with zero mean and a standard deviation of one. For low frequencies, any of them approximates the real $\bar{l}_m(\omega)$ good enough, but, as the frequencies are higher the approximation became poor. In this case, the approximation around the plant bandwidth (2.5386 rad/s) is good for all the data sets. Since the IMC-VRFT as well as the robust test are data-based, the quality of the data is a key issue in the method. Of

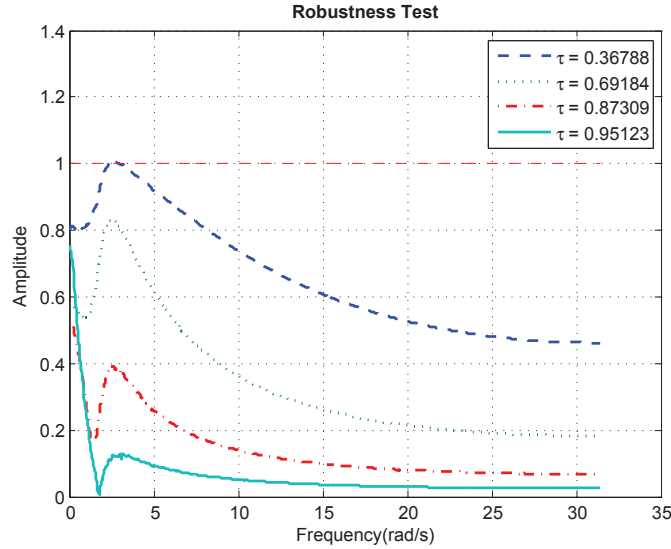


FIGURE 12. Effect on the robust test, for different closed-loop specifications

course, one can not expect to have good approximation of $\bar{l}_m(\omega)$ beyond the maximum frequency component.

6.2. Effect of the selection of the closed-loop transfer function. In this section, the effect of changing the target closed-loop time constant (τ) is addressed. In Figure 12, the robust test is presented for different values. The input data has a bandwidth of 100% of the Nyquist frequency and $Q(z) = q_0$ an the desired closed-loop transfer function is specified as:

$$M(z) = \frac{(1 - \tau)z^{-1}}{1 - \tau z^{-1}} \tag{19}$$

As it can be seen the larger the constant time, the value of the robust test is smaller, i.e., the closed loop is more robust. However, as it can be seen in Figure 14, the step response is worst (less performance). Comparing Figure 12 and Figure 13, it is clear that there is a direct relationship between the approximated $\bar{l}_m(\omega)$ and the difference between the plant and models frequency response. It is obvious that the method is largely affected by the good approximation of the instrumental model to the real plant. For example, since the controller $Q(z)$ is very simple, the instrumental model has the same bandwidth as the desired closed loop, and the closer this desired bandwidth is to the plant bandwidth, the lower is the Integral of the Squared Errors (ISE), as can be seen in Table 4. The ISE is computed for the step response of the controlled system and is computed as:

$$ISE = \frac{1}{t} \sum_{i=1}^t (\text{target}_i - \text{obtained}_i) \tag{20}$$

6.3. Effect of the selection of the number of parameters of $Q(z)$. For this section, a FIR filter with different number of parameters is used. The target closed-loop transfer function is given by (18). The results of this test are presented in Table 5. In this case, as the order of $Q(z)$ is incremented, the robustness of the closed-loop is improved, as presented in Figure 15. In this case, as the controller became more complex, the performance of the controller is also improved, as can be seen in Figure 17, which at the same time, is related with the fact that the instrumental model is very close of the real plant transfer function (see Figure 16).

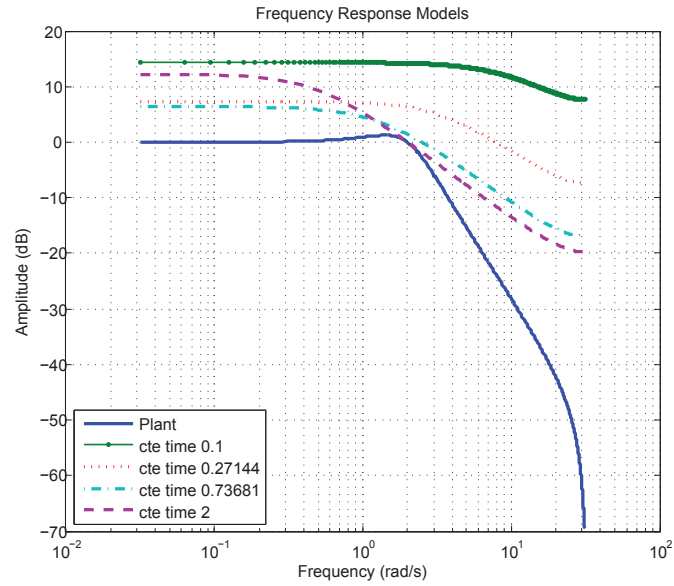


FIGURE 13. Effect on the robust test, for different closed-loop specifications, relationship with the frequency response

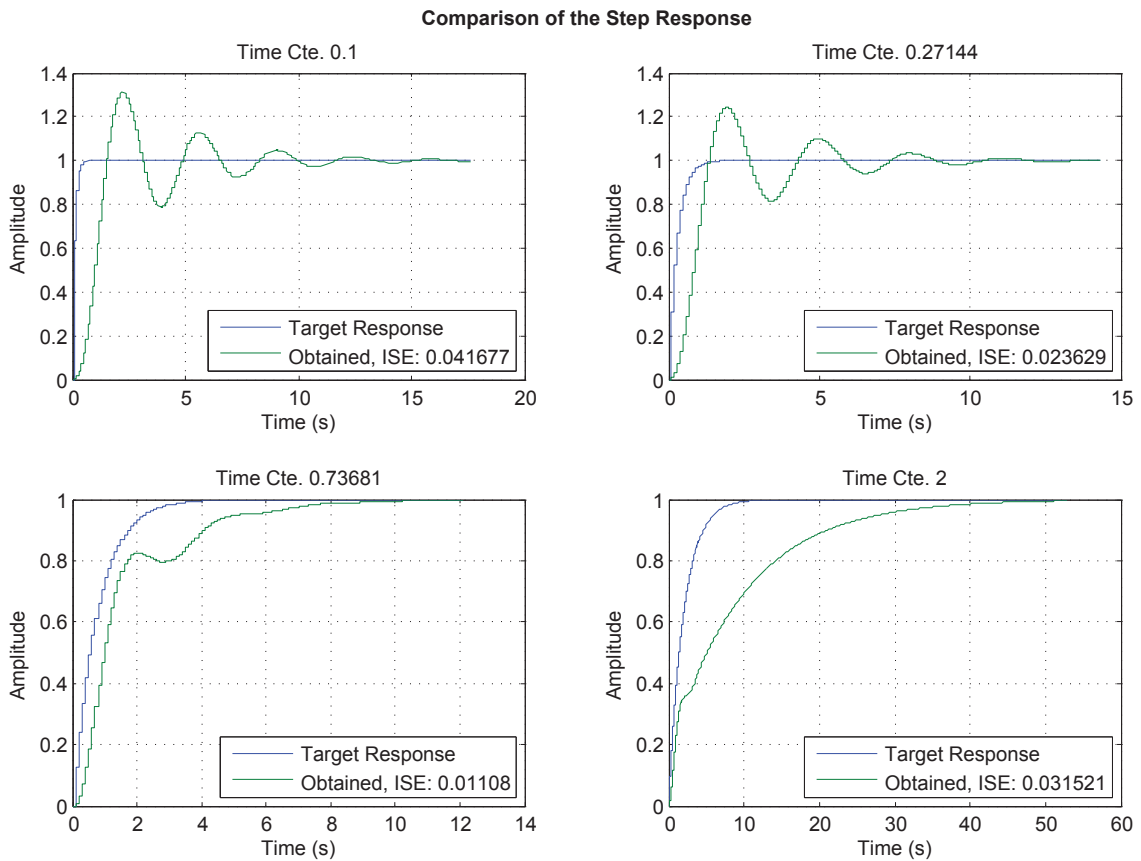


FIGURE 14. Effect on the robust test, for different closed-loop specifications, relationship with the step response

TABLE 4. Effect of the variation of the constant time

Time constant (τ)	Plant bandwidth (rad/s)	Instrumental model bandwidth (rad/s)	Desired bandwidth (rad/s)	Obtained closed-loop bandwidth (rad/s)	ISE
0.36788	2.5386	10.9337	10.9337	2.3687	0.041677
0.69184	2.5386	3.71749	3.71749	2.6131	0.023629
0.87309	2.5386	1.35607	1.35607	0.66615	0.01108
0.95123	2.5386	0.498846	0.498846	0.10463	0.031521

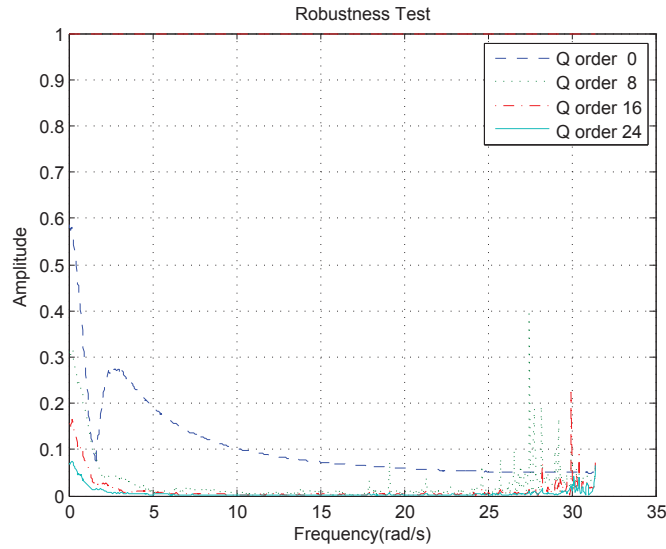


FIGURE 15. Effect on the robust test, for different closed-loop specifications

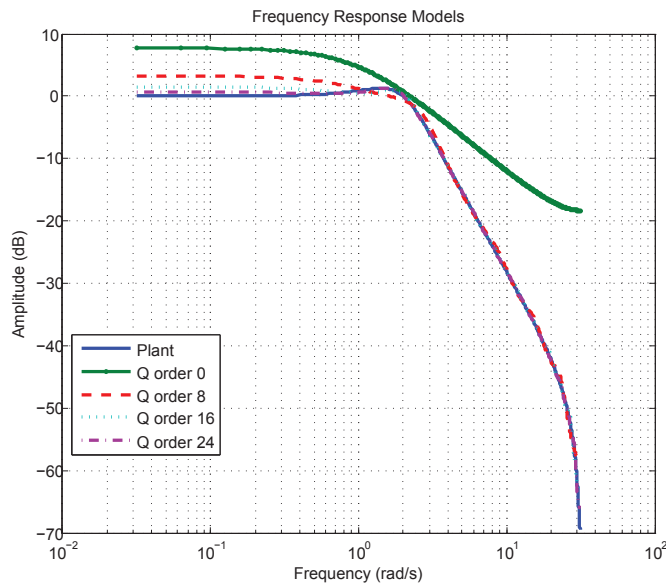


FIGURE 16. Effect on the robust test, for different closed-loop specifications, relationship with the frequency response

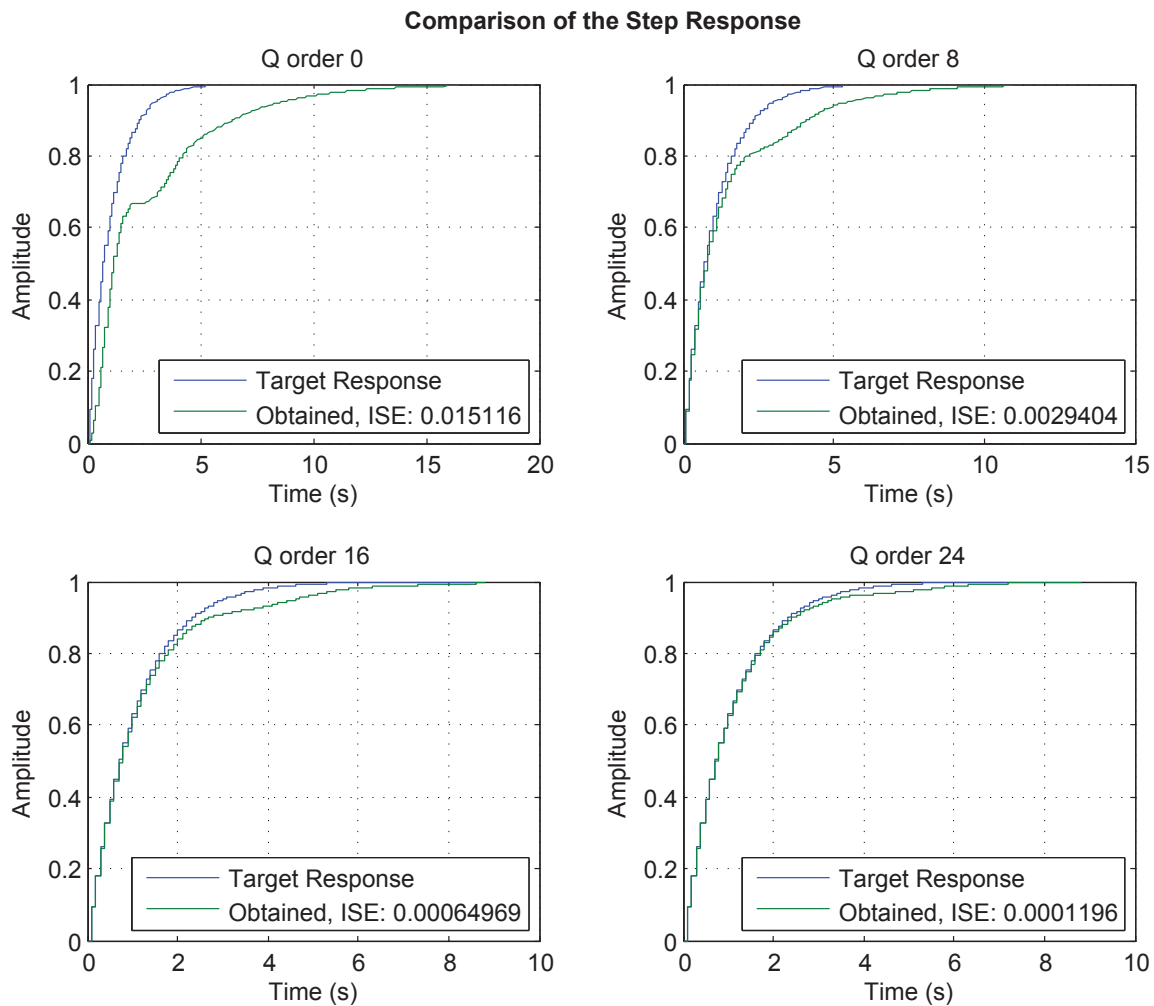


FIGURE 17. Effect on the robust test, for different orders of Q , relationship with the step response

TABLE 5. Effect of the variation of the number of parameters of $Q(z)$

Q order	Plant bandwidth (rad/s)	Instrumental model bandwidth (rad/s)	Desired bandwidth (rad/s)	Obtained closed-loop bandwidth (rad/s)	ISE
0	2.5386	0.99844	0.99844	0.36689	0.015116
8	2.5386	1.4564	0.99844	0.62172	0.0029404
16	2.5386	2.3724	0.99844	0.91801	0.00064969
24	2.5386	2.4053	0.99844	1.0264	0.0001196

7. Conclusion. A new way to tune the IMC controller using a data-driven framework was presented. Taking advantage of the robustness characteristics of the IMC, a robust stability test was conceived to use only data, by approximating the uncertainty function using the ETFE approximation. It was found that this methodology is largely dependent on how good the instrumental model is. This instrumental model is obtained from the optimization of the controller. The approximation of the uncertainty function depends, as it was expected, on the bandwidth of the data.

Acknowledgement. This work has received financial support from the Spanish CICYT program under grant DPI2010-15230. Research work of J. D. Rojas is done under research grant supported by the Universitat Autònoma de Barcelona.

REFERENCES

- [1] H. Hjalmarsson, M. Gevers, S. Gunnarsson and O. Lequin, Iterative feedback tuning: Theory and applications, *Control Systems Magazine, IEEE*, vol.18, no.4, pp.26-41, 1998.
- [2] M. Gevers, A decade of progress in iterative process control design: From theory to practice, *Journal of Process Control*, vol.12, no.4, pp.519-531, 2002.
- [3] A. Karimi, M. Butcher and R. Longchamp, Model-free precompensator and feedforward tuning based on the correlation approach, *Joint IEEE CDC and ECC*, Seville, Spain, 2005.
- [4] M. C. Campi, A. Lecchini and S. M. Savaresi, Virtual reference feedback tuning: A direct method for the design of feedback controllers, *Automatica*, vol.38, no.8, pp.1337-1346, 2002.
- [5] O. Kaneko, S. Soma and T. Fujii, A fictitious reference iterative tuning (FRIT) in the two-degree of freedom control scheme and its application to closed loop system identification, *Proc. of the 16th IFAC World Congress*, Prague, Czech Republic, 2005.
- [6] S. Masuda, M. Kano, Y. Yasuda and G.-D. Li, A fictitious reference iterative tuning method with simultaneous delay parameter tuning of the reference model, *International Journal of Innovative Computing, Information and Control*, vol.6, no.7, pp.2927-2939, 2010.
- [7] Y. Wakasa, K. Tanaka and Y. Nishimura, Application of fictitious reference iterative tuning to shape memory alloy actuators, *ICIC Express Letters, Part B: Applications*, vol.1, no.1, pp.57-62, 2010.
- [8] S. Skogestad, Simple analytic rules for model reduction and PID controller tuning, *Journal of Process Control*, vol.13, no.4, pp.291-309, 2003.
- [9] K. van Heusden, A. Karimi and D. Bonvin, Data-driven model reference control with asymptotically guaranteed stability, *International Journal of Adaptive Control and Signal Processing*, vol.25, no.4, pp.331-351, 2011.
- [10] C. E. Garcia and M. Morari, Internal model control, a unifying review and some new results, *Industrial & Engineering Chemistry Process Design and Development*, vol.21, no.2, pp.308-323, 1982.
- [11] M. Morari and E. Zafirov, *Robust Process Control*, Prentice-Hall International, NJ, USA, 1989.
- [12] I. G. Horn, J. R. Arulandu, C. J. Gombas, J. G. VanAntwerp and R. D. Braatz, Improved filter design in internal model control, *Industrial & Engineering Chemistry Research*, vol.35, no.10, pp.3437-3441, 1996.
- [13] A. Datta and J. Ochoa, Adaptive internal model control: Design and stability analysis, *Automatica*, vol.32, no.2, pp.261-266, 1996.
- [14] D. E. Rivera, M. Morari and S. Skogestad, Internal model control: PID controller design, *Industrial & Engineering Chemistry Process Design and Development*, vol.25, no.1, pp.252-265, 1986.
- [15] R. Vilanova, P. Balaguer, A. Ibeas and C. Pedret, Expected interaction analysis for decentralized control on TITO systems: Application to IMC based PI/PID controller selection, *International Journal of Innovative Computing, Information and Control*, vol.5, no.10(B), pp.3439-3456, 2009.
- [16] A. Aoyama and V. Venkatasubramanian, Internal model control framework using neural networks for the modeling and control of a bioreactor, *Engineering Applications of Artificial Intelligence*, vol.8, no.6, pp.689-701, 1995.
- [17] K. J. Astrom and T. Hagglund, The future of PID control, *Control Engineering Practice*, vol.9, no.11, pp.1163-1175, 2001.
- [18] G. O. Guardabassi and S. M. Savaresi, Virtual reference direct design method: An off-line approach to data-based control system design, *IEEE Transactions on Automatic Control*, vol.45, no.5, pp.954-959, 2000.
- [19] A. Lecchini, M. C. Campi and S. M. Savaresi, Sensitivity shaping via virtual reference feedback tuning, *Proc. of the 40th IEEE Conference on Decision and Control*, vol.1, pp.750-755, 2001.
- [20] A. Lecchini, M. C. Campi and S. M. Savaresi, Virtual reference feedback tuning for two degree of freedom controllers, *International Journal of Adaptive control and Signal Processing*, vol.16, no.5, pp.355-371, 2002.
- [21] J. D. Rojas and R. Vilanova, Feedforward based two degrees of freedom formulation of the virtual reference feedback tuning approach, *Proc. of the European Control Conference*, Budapest, Hungary, pp.1800-1805, 2009.
- [22] A. Sala and A. Esparza, Extensions to “virtual reference feedback tuning: A direct method for the design of feedback, controllers”, *Automatica*, vol.41, no.8, pp.1473-1476, 2005.

- [23] S. Skogestad and I. Postlethwaite, *Multivariable Feedback Control, Analysis and Design*, 2nd Edition, John Wiley & Sons, West Sussex, England, 2007.
- [24] K. van Heusden, A. Karimi and D. Bonvin, Data-driven controller tuning with integrated stability constraint, *The 47th IEEE Conference on Decision and Control*, Cancun, Mexico, pp.2612-2617, 2008.
- [25] L. Ljung, *System Identification, Theory for the User*, 2nd Edition, Prentice Hall, 1999.
- [26] E. Feron, M. Brenner, J. Paduano and A. Turevskiy, Time-frequency analysis for transfer function estimation and application to flutter clearance, *Journal of Guidance, Control, and Dynamics*, vol.21, no.3, pp.375-382, 1998.
- [27] A. Stenman, F. Gustafsson, D. E. Rivera, L. Ljung and T. McKelvey, On adaptive smoothing of empirical transfer function estimates, *Control Engineering Practice*, vol.8, no.11, pp.1309-1315, 2000.
- [28] A. Stenman and F. Gustafsson, Adaptive smoothing methods for frequency-function estimation, *Automatica*, vol.37, no.5, pp.675-685, 2001.
- [29] F. Badran, M. Crépon, C. Mejia, S. Thiria and N. Tran, Empirical transfer function determination by the use of multilayer perceptron, *Neurocomputing*, vol.30, no.1-4, pp.31-35, 2000.
- [30] Y. Kansha, Y. Hashimoto and M.-S. Chiu, New results on VRFT design of PID controller, *Chemical Engineering Research and Design*, vol.86, no.8, pp.925-931, 2008.